

# Study of the Two-Gap Superconductivity in GdO(F)FeAs by ScS-Andreev Spectroscopy

T.E. Shanygina<sup>1,2</sup>, Ya.G. Ponomarev<sup>2</sup>, S.A. Kuzmichev<sup>2</sup>,  
M.G. Mikheev<sup>2</sup>, S.N. Tchesnokov<sup>2</sup>, O.E. Omel'yanovsky<sup>1</sup>,  
A.V. Sadakov<sup>1</sup>, Yu.F. Eltsev<sup>1</sup>, V.M. Pudalov<sup>1</sup>, A.S. Usol'tsev<sup>1,2</sup>,  
E.P. Khlybov<sup>3</sup>, and L.F. Kulikova<sup>3</sup>

<sup>1</sup> P.N. Lebedev Physical Institute, 119991 Moscow, Russia

<sup>2</sup> M.V. Lomonosov Moscow State University, 119991 Moscow, Russia

<sup>3</sup> Institute for High Pressure Physics, 142190 Troitsk, Russia

E-mail: tatiana.shanygina@gmail.com

**Abstract.** Current-voltage characteristics and dynamic conductance of the superconductor - constriction - superconductor junctions in GdO(F)FeAs polycrystalline samples with critical temperatures  $T_C^{\text{local}} = 46 \div 53$  K were investigated. Two superconducting gaps, the large  $\Delta_L = 10.5 \pm 2$  meV, and the small one  $\Delta_S = 2.3 \pm 0.4$  meV were clearly observed at  $T = 4.2$  K. The  $2\Delta_L/k_B T_C^{\text{local}} = 5.5 \pm 1$  ratio gives support to the strong coupling mechanism which is responsible for the high  $T_C$  value. Temperature dependence of the large gap  $\Delta_L(T)$  indicates the presence of intrinsic proximity effect (in  $k$ -space) between two superconducting condensates.

Novel Fe-based superconductors [1] are now in the focus of intensive experimental research. Some of their features such as layered crystal structure and spatial separation of superconducting layers are similar to those of cuprates and MgB<sub>2</sub>. The stoichiometric 1111-family compounds were shown to be antiferromagnetic metals with spin density wave (SDW) ground state [2, 3]. Partial oxygen deficiency or fluorine substitution for oxygen induces superconductivity in the Fe-As layers. Rare-earth elements replacement also affects the critical temperature  $T_C$ . In particular,  $T_C$  for Gd-1111 oxypnictides can be lowered by replacement of Y for Gd [4] or increased by introducing Th instead of Gd [5]. The  $T_C = 56$  K reported in Gd<sub>0.8</sub>Th<sub>0.2</sub>FeAs compound is today the highest one for Fe-based superconductors.

Band-structure calculations showed the total density of states  $N(0)$  at the Fermi level to be formed mainly by Fe  $3d$ -states [6, 7, 8]. A large Fe-isotope effect [9] and the correlation between  $T_C$  and  $N(0)$  for different iron-based superconductors [10] give support to the phonon-mediated coupling in these compounds. The theoretically calculated Fermi surface for 1111-system compounds [11, 12, 13, 14] comprises cylinder-like hole sheets centered at the  $\Gamma$  point and quasi-two-dimensional (2D) electron sheets at the  $M$  point of the reduced Brillouin zone.

Here we present the superconducting gap measurements in GdO(F)FeAs by Andreev spectroscopy of ScS-contacts (superconductor - constriction - superconductor) using a “break-junction” technique.

Nearly optimally doped Gd-1111 samples were prepared by high pressure synthesis described in detail in [15, 16]. Superconducting properties of the samples were tested by measuring temperature dependences of the AC-magnetic susceptibility and resistance  $R(T)$ . Both showed

a sharp superconducting transition at  $T_C^{\text{bulk}} = (52 \div 53) \text{ K}$  (the bulk value of the critical temperature was defined at the maximum of  $dR(T)/dT$ -curve). The two sets of polycrystalline GdO(F)FeAs samples were studied: “El”-series ( $\text{GdO}_{0.88}\text{F}_{0.12}\text{FeAs}$ ,  $T_C^{\text{bulk}} = 53 \pm 1 \text{ K}$ ) and “Kh”-series ( $\text{GdO}_{0.91}\text{F}_{0.09}\text{FeAs}$ ,  $T_C^{\text{bulk}} = 52 \pm 1 \text{ K}$ ). Figure 1 shows typical temperature dependences of resistance for Kh-series samples.

In order to determine superconducting gap values for GdO(F)FeAs, we used (i) Andreev spectroscopy [17] of individual Sharvin-type [18] ScS-contacts and (ii) intrinsic Andreev spectroscopy (intrinsic multiple Andreev reflections effect (IMARE) [19], which usually exists due to the presence of steps and terraces at clean cryogenic clefts). ScS-Andreev nanocontacts in polycrystalline samples were prepared by the “break-junction” technique [20, 21]. The samples of the typical size  $1.5 \times 0.5 \times 0.1 \text{ mm}^3$  were attached to the flexible sample holder with two current and two potential leads by In-Ga alloy that is liquid at room temperature. The holder with the sample was cooled down to 4.2 K, then a microcrack in the sample was generated by precise bending the sample holder.

The resulting nano-contact is a mechanical contact of two clean cryogenically cleaved surfaces separated by a constriction; this geometry excludes impurity presence at the cryogenic clefts. The  $I(V)$ -,  $dI(V)/dV$ -characteristics of the contact were measured using a standard AC-modulation technique [22, 23].

According to the theory by Kümmel *et al.* [24] for the SnS (superconductor - normal metal - superconductor) Andreev-type contact, the main features of its current-voltage characteristics (CVC) are the excess current at low bias voltages and the subharmonic gap structure (SGS). The latter shows series of dynamic conductance dips at bias voltages

$$V_n = \frac{2\Delta}{en}, \quad n = 1, 2, \dots \quad (1)$$

due to the multiple Andreev reflections effect. For a multigap superconductor, several independent SGSs corresponding to each gap should be observed. The CVCs studied in this work are typical for the clean classical SnS-contact (with a constriction acting as a normal metal) with excess-current at low bias voltage, therefore, we believe, the theoretical model by Kümmel *et al.* [24] is applicable to our break-junctions. Strictly speaking, the sharpest SGS are intrinsic of Andreev contacts of the highest quality with a small diameter  $a$  which is less than the quasiparticles mean free path  $l$  (i.e., in the ballistic limit) [18]. In such a case one may observe a large number of gap peculiarities, thus facilitating the gap energy measurements. In the case  $a \approx l$ , only few SGS minima would contribute to the dynamic conductance spectra, which in most cases corresponds to the studied GdO(F)FeAs ScS-contacts.

In the framework of the “break-junction” technique and due to the layered structure of GdO(F)FeAs, the so-called stacks of Andreev contacts may be formed on cryogenic clefts; this type of junctions, the  $S - c - \dots - S - c - S$ -array, enables one to observe IMARE similar to that observed earlier in Bi-2201 [25]. For such an array, bias voltage for any peculiarities caused by the bulk properties at  $dI(V)/dV$ -characteristic scales with number of sequentially connected contacts  $N$  as compared with the single junction case. On the contrary, this is not the case for such CVC features that originate from any defects influence on the cleaved surfaces. One can determine  $N$  by collating dynamic conductance spectra of Andreev arrays with different number of junctions in a stack and normalizing them to a single contact characteristics. The array contacts are a factor of  $N$  less sensitive to surface defects (which otherwise would seriously affect the properties of superconductor [26]). Thus, by making CVC measurements on the stack contacts, one can determine the *true bulk gap* values much more accurately.

Figure 2 shows dynamic conductance of two ScS-Andreev contacts: single junction El3d1, lower black line, and an array Kh3d4, upper gray line. After normalizing the  $dI(V)/dV$ -characteristic of the array ( $N = 2$  for this case) to that for the single junction, we achieve a good

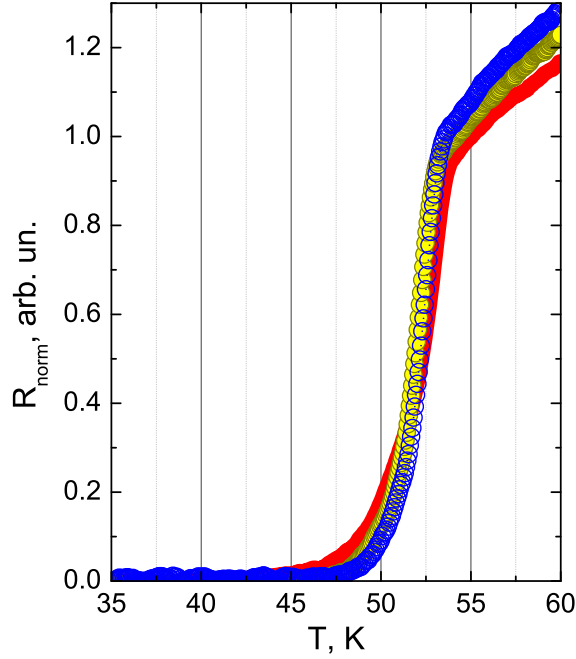


**Figure 1.** Normalized temperature dependence of resistance for polycrystalline  $\text{GdO}_{0.91}\text{FeAs}$  samples Kh1 (solid yellow circles), Kh2 (red line) and Kh3 (open blue circles) measured prior a microcrack formation. The bulk critical temperatures  $T_C^{\text{bulk}} = 52 \pm 1$  K.

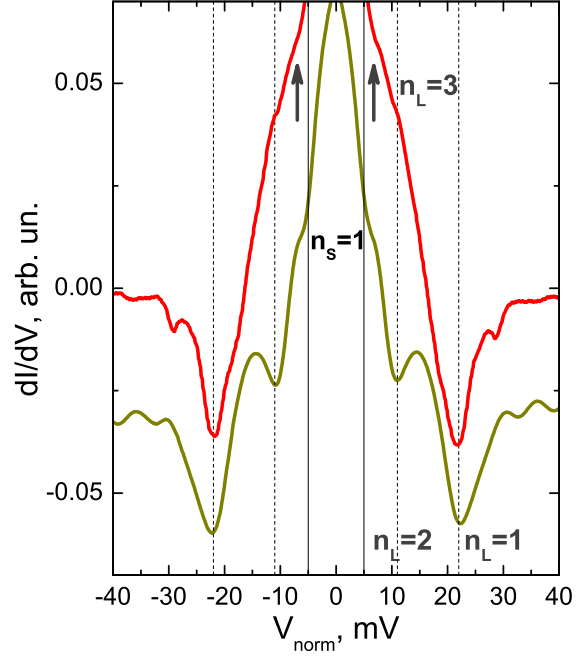


**Figure 2.**  $dI/dV$ -curves for the single-junction ScS-contact El1d6 (lower yellow line) and 2-junctions Kh3d4 array (normalized to a single junction; upper red line).  $T = 4.2$  K. SGS dips defining  $\Delta_L \approx 11$  meV and  $\Delta_S \approx 2.5$  meV are marked with  $n_L$  and  $n_S$  labels, respectively.

coincidence of the spectra peculiarities. Such a procedure was done for all ScS-arrays, with  $N$  as a fitting parameter. The normalized dynamic conductance shows a set of dips at bias voltages  $V \approx 22$  mV and 11 mV (marked by dashed vertical lines). The minimum at  $V \approx 7.3$  mV is seen only at the Kh3d4-curve (marked by arrows) for stack contact. These three peculiarities may be associated with the SGS minima  $n_L = 1, 2, 3$ , which leads to the estimated local value of the large superconducting gap  $\Delta_L \approx 11$  meV. The minima at  $V \approx \pm 5$  mV at the El1d6-curve (marked by solid vertical lines) don't correspond to the expected bias voltage  $V \approx 7.3$  mV for the 3rd harmonic  $n_L = 3$  of the large gap, and, hence, indicates the presence of the small gap  $\Delta_S \approx 2.5$  meV. The satellite minima above the  $n_L = 1$  dips may originate from excitation of Leggett collective modes and require additional studies.

For some contacts (such as El3 sample, single ScS-Andreev junction #d1), one can see the SGS originating from the small gap, but not only a single peculiarity. Figure 3 shows such series comprising  $n_S = 1, 2, 3$  at  $V \approx (4.4, 2.2, 1.3)$  mV (vertical dashed lines). Using eq. (1), we directly find the small superconducting gap value  $\Delta_S \approx 2.2$  meV. The additional fine structure seen in Fig. 3 at  $V \approx 5$  mV may be caused by the  $\Delta_S$  order parameter anisotropy and is subject of further studies. As the small gap SGS is located near zero bias voltages, it becomes smeared by the dramatic increasing of the dynamic conductance at the  $dI/dV$ -curve. Hence, the background subtraction or taking the second derivative of the CVC helps one to distinguish the small gap peculiarities, as was done to the spectrum at the Fig.3.

By a precise mechanical readjusting of the contact, we were able to observe characteristics of several ScS break-junctions within the same low-temperature experiment; the independent

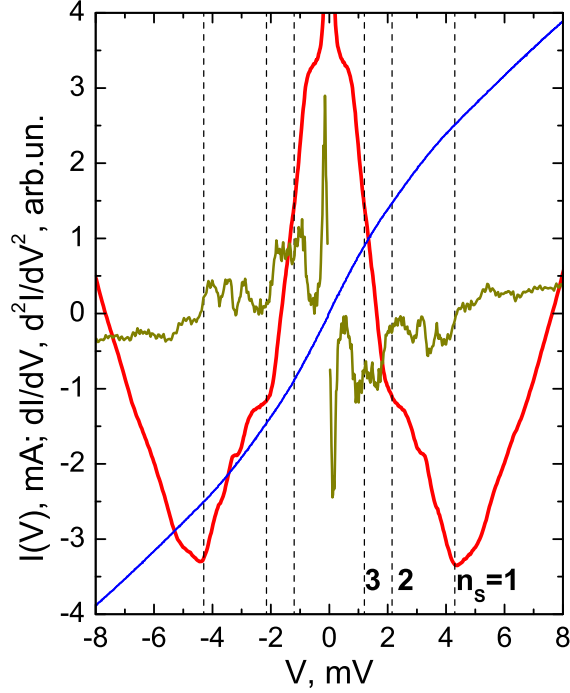


**Figure 3.**  $I(V)$ - (blue line),  $dI/dV$ - (red line) and  $d^2I/dV^2$ -characteristics (yellow line) for single ScS-contact El3d1.  $T = 4.2$  K. The SGS dips associated with small gap  $\Delta_S \approx 2.2$  meV are marked by dashed vertical lines. Linear background is subtracted.

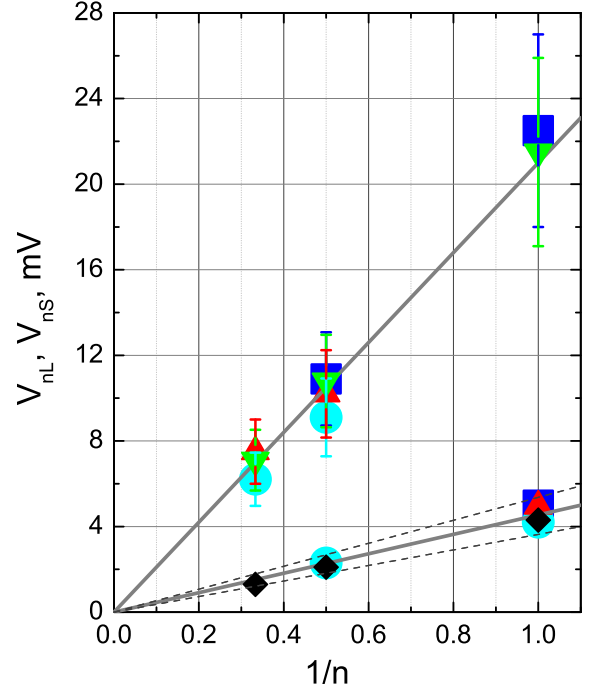


**Figure 4.** Normalized to a single junction SGS bias voltages  $V_{nL}$ ,  $V_{nS}$  versus  $1/n$  for several ScS-contacts ( $T_C = 46 \div 53$  K) investigated. The solid lines indicate the averaged gap values  $\Delta_L = 10.5 \pm 2$  meV and  $\Delta_S = 2.3 \pm 0.4$  meV at  $T = 4.2$  K.

local gap measurements improve the statistics of the results. To get values of  $\Delta_{L,S}$  and their scatter, in accordance with eq. (1), we plotted SGS minima positions  $V_n$  as a function of their inverse number  $1/n$ ; this line should start at the (0,0) point. Our experimental data measured at  $T = 4.2$  K are summarized on Figure 4 that shows the results for three samples with a similar  $T_C^{\text{bulk}}$  (Kh3d4 contact - down triangles, El1d6 - squares, El3d1 - rhombs, El3d2 - circles, and El3d13 - up triangles). All the data agree with each other and confirm the presence of the two distinct superconducting gaps. The averaged gap values obtained at  $T = 4.2$  K [16, 27] are:

$$\Delta_L = 10.5 \pm 2 \text{ meV}, \Delta_S = 2.3 \pm 0.4 \text{ meV}$$

for the critical temperatures  $T_C^{\text{local}} = (46 \div 53)$  K. The close agreement of the data for various samples shows the reproducibility of the measured gaps magnitude.

IMARE spectroscopy technique also facilitates measurements of temperature dependence of the superconducting gaps. The subharmonic gap structure of the dynamic conductance of symmetrical SnS-contacts remains rather well-pronounced up to  $T_C$ . Importantly, to define the gap value no additional fitting is required [24]: at any temperatures up to  $T_C$  the gap  $\Delta$  can be obtained straightforward using the expression (1). We note, that in case of alternative technique of the Andreev spectroscopy of SN-junctions, and for a two-gap superconductor, one needs to fit the resulting conductance curves using 7 fitting parameters.

Figure 5 shows the dynamic conductance of ScS-array (sample Kh3, contact #d4, see Fig. 2) measured in the range  $4.2 \text{ K} \leq T \leq T_C$ . The curves are shifted vertically for clarity. The

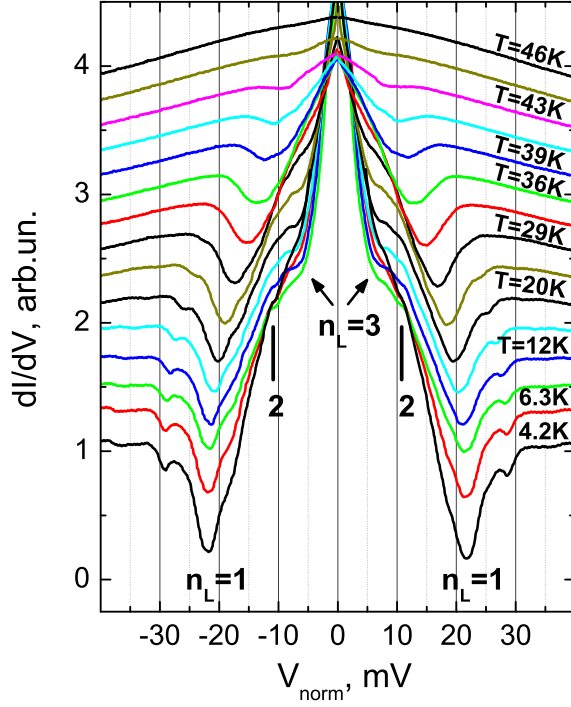


**Figure 5.** The temperature affecting on the SGS (black labels) at normalized dynamic conductance of 2 ScS-junctions array Kh3d4 ( $4.2\text{ K} \leq T \leq T_C$ ).  $\Delta_L(4.2\text{ K}) \approx 11\text{ meV}$ . Local critical temperature  $T_C^{\text{local}} \approx 46\text{ K}$ . The curves were shifted along the vertical scale for the sake of clarity.

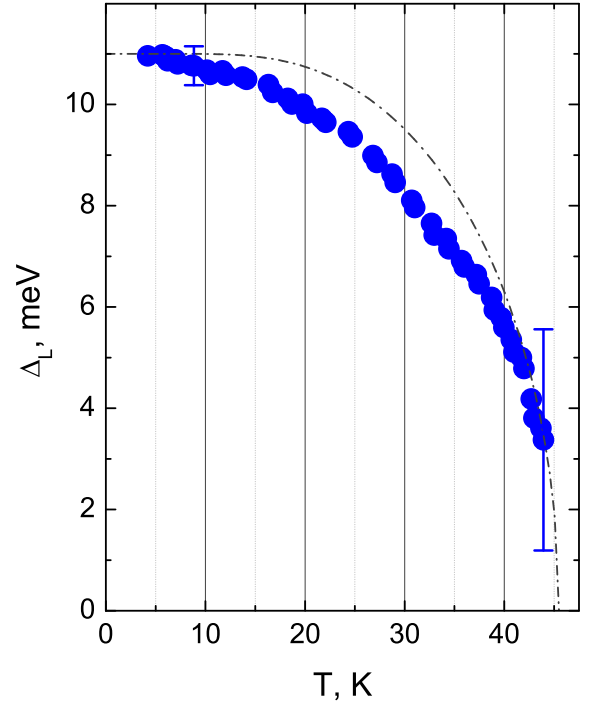


**Figure 6.** Temperature dependence of the large gap  $\Delta_L(T)$  (circles) plotted under the data of Figure 5.  $T_C^{\text{local}} \approx 46\text{ K}$ . Single-gap BCS-like behavior (dash-dotted line) is presented for comparison. Error bars show typical temperature smearing for Cooper pairs at two representative temperatures.

peculiarities are washed out at  $T_C^{\text{local}} \approx 46\text{ K}$ . The “local” critical temperature is referred to as the temperature of the transition to the normal state in the contact area (with diameter  $a \approx l$ ). It is worthy to note that the  $T_C^{\text{local}}$  can differ from the  $T_C^{\text{bulk}}$ , the averaged characteristic measured by non-local methods. The coincidence of the local  $T_C^{\text{local}}$  and the averaged  $T_C^{\text{bulk}}$  may be observed only in the ideal clean and homogeneous sample. By taking the  $\Delta_L \approx 11\text{ meV}$  value (see Fig. 2) and  $T_C^{\text{local}} \approx 46\text{ K}$  from Figure 5, for the Kh3d4 array we obtain an estimate for the BCS ratio,  $2\Delta_L/k_B T_C^{\text{local}} \approx 5.5$ ; the ratio would however be reduced to 4.8 if we use the averaged  $T_C^{\text{bulk}} = 53 \pm 1\text{ K}$  value, as in Refs. [16, 27]. The former value 5.5 is close to that for  $\text{LaO}_{0.9}\text{F}_{0.1}\text{FeAs}$  (a lower- $T_C$  analogue of Gd-1111) [28]. At the same time, the measured  $2\Delta_L/k_B T_C^{\text{local}}$ -ratio exceeds the standard single-gap BCS value 3.52 for the weak coupling limit. Presumably, the  $2\Delta_L/k_B T_C$  value suggests the strong coupling in the condensates with a large gap value. As for the small gap, our data leads to  $2\Delta_S/k_B T_C = 1.1 \div 1.3$  which is less than the BCS value 3.52.

Figure 6 shows the temperature dependence of the large gap  $\Delta_L(T)$  obtained from our IMARE measurements (see Fig. 5) within the range  $4.2\text{ K} \leq T \leq T_C^{\text{local}}$ . Similar measurements of the temperature dependence for the small gap represent a harder task, possibly require higher quality of samples, and have not been accomplished yet. The  $\Delta_L(T)$  dependence lies noticeably below the standard single-gap BCS-like curve (dash-dotted line in Figure 6). Note that the temperature smearing (see error bars plotted for the last data point) allows to resolve the gap value up to  $\approx 44.5\text{ K}$ . The deviation in the  $\Delta_L(T)$  dependence could not be attributed to surface gap influence



(i.e., it is not due to the real space proximity effect), because it is obtained from Andreev reflection measurements in the *array* contact, where the surface effects are reduced. Moreover, the  $\Delta_L(T = 0)$  energy coincides with the value for the single ScS-contacts (see Fig. 2, 4). Were the real-space proximity effect be responsible for the deviation, the  $\Delta_L(T = 0)$  would differ; our experiment, however, shows this is not the case. Such behavior resembles the  $\Delta_\sigma(T)$ -dependence for  $\text{MgB}_2$  [29, 30, 31] and  $\Delta_L(T)$  for  $\text{FeSe}$  [23]. Theoretical studies [32, 33, 34] explain such a deviation by interband coupling effect. By analogy, we assume that similar deviation for Gd-1111 may arise from nonzero interband coupling. The reduced BCS-ratio for the small gap also supports this conclusion and suggests that the “weak” superconductivity in the low gap condensate may be induced by  $k$ -space (internal) proximity effect between two superconducting condensates [35]. According to Refs. [32, 33, 34], the observed shape of the  $\Delta(T)$  curve (see Figure 6) is typical for the “driving” condensate in the presence of the second (driven) condensate with a small gap.

The existence of the large superconducting gap ( $2\Delta_L/k_B T_C^{\text{bulk}} > 4$ ) in the 1111-family compounds with critical temperatures  $40 \text{ K} \leq T_C \leq 53 \text{ K}$  was confirmed by tunneling spectroscopy (“break-junction” technique) [36, 37], point-contact Andreev reflection (PCAR) spectroscopy of SN-junctions [38, 39, 40, 41, 42, 43, 44], and angle-resolved photoemission spectroscopy (ARPES) [45]. To the best of our knowledge, there are no other data available for Gd-1111 to compare with. Thus, comparing our results for  $\text{GdO}(\text{F})\text{FeAs}$  with the aforementioned data on other 1111-superconductors, we find rather good agreement with  $2\Delta_L/k_B T_C$  values determined by “break-junction” technique [36, 37] and in some PCAR-measurements [43, 44].

In conclusion, we studied the dynamic conductance of ScS-contacts in  $\text{GdO}_{1-x}\text{F}_x\text{FeAs}$  ( $x = 0.09, 0.12$ ) polycrystalline samples ( $T_C^{\text{local}} = 46 \div 53 \text{ K}$ ) by ScS Andreev spectroscopy, in the temperature range  $4.2 \text{ K} \leq T \leq T_C$ . We detected two superconducting gaps, the large  $\Delta_L = 10.5 \pm 2 \text{ meV}$ , and the small  $\Delta_S = 2.3 \pm 0.4 \text{ meV}$ . The observed temperature dependence of the large gap  $\Delta_L(T)$  suggests the existence of  $k$ -space proximity effect between two superconducting condensates and, therefore, nonzero interband interaction. The estimated  $2\Delta_L/k_B T_C^{\text{local}} = 5.5 \pm 1$  ratio exceeds the BCS limit 3.52 and indicates the strong coupling regime in the “driving” condensate.

The work was supported by grants from RFBR, and the Russian Ministry of Education and Science. We also thank A. Bianconi and A. Kordyuk for appreciation and valuable discussions.

## References

- [1] Kamihara Y *et al.* 2008 *J. Am. Chem. Soc.* **130** 3296
- [2] Klauss H H *et al.* 2008 *Phys. Rev. Lett.* **101** 077005
- [3] Luetkens H *et al.* 2008 *Phys. Rev. Lett.* **101** 097009
- [4] Kadowaki K *et al.* 2009 *J. Phys.: Conf. Ser.* **83** 67006
- [5] Wang C *et al.* 2008 *Europhys. Lett.* **150** 052088
- [6] Nekrasov I A *et al.* 2008 *JETP Lett.* **87** 560
- [7] Eschrig H and Koepernik K 2009 *Phys. Rev. B* **80** 104503
- [8] Miyake T *et al.* 2010 *J. Phys. Soc. Jpn.* **79** 044705
- [9] Liu R H *et al.* 2009 *Nature* **459** 64
- [10] Sadovskii M V *et al.* 2010 *JETP Lett.* **91** 518
- [11] Singh D J and Du M H 2008 *Phys. Rev. Lett.* **100** 237003
- [12] Singh D J 2009 *Physica C* **469** 418
- [13] Nekrasov I A *et al.* 2008 *JETP Lett.* **88** 144
- [14] Coldea A I *et al.* 2008 *Phys. Rev. Lett.* **101** 216402
- [15] Khlybov E P *et al.* 2009 *JETP Lett.* **90** 387
- [16] Shanygina T E *et al.* 2011 *JETP Lett.* **93** 94
- [17] Andreev A F 1964 *Sov. Phys. JETP* **19** 1228
- [18] Sharvin Yu V 1965 *Zh. Eksp. Teor. Fiz.* **48** 984
- [19] Nakamura H *et al.* 2009 *J. Phys. Soc. Jpn.* **78** 123712
- [20] Moreland J and Ekin J W 1985 *J. Appl. Phys.* **58** 3888

- [21] Müller J *et al.* 1992 *Physica C* **191** 485
- [22] Ponomarev Ya G and Rakhmanina A V 1970 *Prib. Tehn. Eksp.* **5** 120
- [23] Ponomarev Ya G *et al.* 2011 *Zh. Eksp. Teor. Fiz.* **140** 527
- [24] Kümmel R *et al.* 1990 *Phys. Rev. B* **42** 3992
- [25] Ponomarev Ya G *et al.* 2000 *Inst. Phys. Conf. Ser.* **167** 241
- [26] van Heumen E *et al.* 2011 *Phys. Rev. Lett.* **106** 027002
- [27] Pudalov V M *et al.* 2011 *Physics-Uspekhi* **54** 648
- [28] Ponomarev Ya G *et al.* 2009 *Phys. Rev. B* **79** 224517
- [29] Ponomarev Ya G *et al.* 2004 *Solid State Comm.* **129** 85
- [30] Ponomarev Ya G *et al.* 2004 *JETP Lett.* **79** 484
- [31] Kuzmichev S A *et al.* 2012 *Solid State Comm.* **152** 119
- [32] Moskalenko V A 1959 *Phys. Met. Metall.* **4** 503
- [33] Suhl H *et al.* 1959 *Phys. Rev. Lett.* **12** 552
- [34] Nicol E J and Carbotte J P 2005 *Phys. Rev. B* **71** 054501
- [35] Yanson I K *et al.* 2003 *Phys. Rev. B* **67** 024517
- [36] Ekino T *et al.* 2009 *Physica C* **470** S358
- [37] Sugimoto A *et al.* 2010 *Physica C* **470** 1070
- [38] Daghero D *et al.* 2009 *Phys. Rev. B* **80** 060502(R)
- [39] Gonnelli R S *et al.* 2009 *Physica C* **469** 512
- [40] Wang Y L *et al.* 2009 *Supercon. Sci. Technol.* **22** 015018
- [41] Miyakawa N *et al.* 2010 *J. Supercond. Novel Magn.* **23** 575
- [42] Tanaka M and Shimada D 2010 *J. Supercond. Novel Magn.* **24** 1491
- [43] Yates K A *et al.* 2009 *New J. Phys.* **11** 025015
- [44] Samuely P *et al.* 2009 *Supercon. Sci. Technol.* **22** 014003
- [45] Kondo T *et al.* 2008 *Phys. Rev. Lett.* **101** 147003